



## OPEN ACCESS

# Search for QGP and thermal freeze-out of strange hadrons

To cite this article: Giorgio Torrieri and Johann Rafelski 2001 *New J. Phys.* **3** 12

View the [article online](#) for updates and enhancements.

## You may also like

- [Maximum mass of charged strange quark star in presence of strange quark mass \( \$m\_s\$ \)](#)  
A Saha, K B Goswami, R Roy et al.
- [Identified particle spectra in Pb–Pb, Xe–Xe and p–Pb collisions with the Tsallis blast-wave model](#)  
Guorong Che, Jinbiao Gu, Wenchao Zhang et al.
- [Strangeness production with ALICE at the LHC](#)  
Maria Vasileiou and On behalf of the ALICE Collaboration

## Search for QGP and thermal freeze-out of strange hadrons

**Giorgio Torrieri and Johann Rafelski**

Department of Physics, University of Arizona, Tucson, AZ 85721, USA

E-mail: [torrieri@physics.arizona.edu](mailto:torrieri@physics.arizona.edu) and

[rafelski@physics.arizona.edu](mailto:rafelski@physics.arizona.edu)

*New Journal of Physics* **3** (2001) 12.1–12.17 (<http://www.njp.org/>)

Received 8 January 2001, in final form 4 June 2001

Published 22 June 2001

**Abstract.** After reviewing the observables of QGP we perform an analysis of  $m_{\perp}$  spectra of strange hadrons measured as function of centrality in 156 A GeV Pb–Pb interactions. We show that there is a good agreement between the chemical and thermal freeze-out conditions, providing additional evidence for the formation and sudden disintegration of a supercooled QGP fireball.

### 1. Quark matter in the laboratory

The development of the quark model has been from the first accompanied by consideration of the transition from a few-body hadronic bound state to a many-body quark matter star formation [1]. This was followed by the development of the quantum many-body theory of quark matter [2, 3], which led on to the formal recognition within the framework of QCD that the perturbative quark matter state must exist [4], given the asymptotically free nature of the theory of strong interactions, quantum-chromodynamics (QCD). Arguments arising from study of a dense hadron gas within the scheme of Hagedorn's statistical bootstrap and the resulting boiling of hadronic matter lead from a different direction to the consideration of the transition to a hadron substructure phase [5]. In short, the quark gluon plasma (QGP), which we today call hot quark matter, has been an expected new state of matter for 30 years.

The nuclear physics establishment considered at that time, if not still today, other ideas about new phases of matter which could be formed in relativistic nuclear collisions to be of greater interest. It is interesting to recall here that in the first of the series of formative workshops in the field of relativistic heavy-ion collisions, the 'Bear Mountain' meeting of November 1974, there is not a single mention of quarks, let alone of quark matter. At the time 'Lee–Wick' ultra dense nuclei, pion condensates and multi-hyperon nuclear states were considered as the potential discoveries of these new and coming tools of nuclear physics research.

As the ideas about QGP formation in high-energy nuclear collisions matured [6], a challenge emerged as to how the locally deconfined state which exists for a mere  $10^{-22}$  s can be distinguished from the gas of confined hadrons. This is also a matter of principle, since arguments were advanced that this might be impossible since both quark and hadron pictures of the reaction are equivalent. Therefore a quark–gluon based description is merely a change of Hilbert space expansion basis.

Clearly these difficult questions can be settled by an experiment, if a probe of the QGP operational on the collision time scale can be devised. There were three major groups of observables proposed, and we address these in the chronological order of their appearance in the literature.

### *1.1. Dileptons, direct photons*

The study of multi-particle production phenomena has stimulated the exploration of dileptons and photons as the probe of dense hadron matter fireballs, which ideas were easily adapted to the QGP phase situation. After the seminal work of Feinberg [7] and Shuryak [8] a comprehensive discussion of this observable was offered [9].

However, since electromagnetic currents are the source of photons and dileptons, both confined and deconfined dense elementary hadron matter can produce these electromagnetic probes. The principal novel component of QGP, gluons, is not a required ingredient.

On the practical side, the backgrounds are very significant. The photon production is dominated by factor 10–20 larger  $\pi^0$  decay, and dileptons arise in decays of vector mesons which are also abundantly produced in multi-particle production processes, irrespective of whether the formation of QGP has occurred or not. Thus the electromagnetic signature of QGP has to be extracted by comparing in a detailed and quantitative study experiment with theory.

Such a comparison is extremely difficult unless we have good data and already know at what condition QGP has been formed and how it evolved. But present day experiments suffer both from systematic acceptance issues, and low statistics. In our view, the electromagnetic probes will come of age as second-generation diagnostic tools in the refinement of the study of the QGP phase properties.

### *1.2. Strangeness enhancement*

One aspect of this probe of QGP will be addressed in this paper. The ideas about enhancement are simple: when colour bonds are broken the chemically (abundance) equilibrated deconfined state has an unusually high abundance of strange quarks [10]. Subsequent study of the dynamical process of chemical equilibration has shown that only the gluon component in the QGP is able to produce strangeness rapidly [11], allowing formation of a (nearly) chemically equilibrated dense phase of deconfined, hot, strangeness-rich, quark matter in relativistic nuclear collisions. Therefore strangeness enhancement is related directly to the presence of gluons in QGP.

The high density of strangeness formed in the reaction fireball favours formation of multi-strange hadrons [12, 13], which are produced rarely if only individual hadrons collide [14, 15]. In particular, a large enhancement of multi-strange antibaryons has been proposed as a characteristic and nearly background-free signature of QGP [12]. Such a systematic enhancement has in fact been observed, rising with strangeness content [16].

Although conventional theoretical models were explored to interpret the strangeness signatures of new physics [17], we are not aware of a consistent interpretation of the data other than in the context of QGP formation. Experimental results are abundant and allow a precise diagnosis of the chemical freeze-out conditions [18], and an assessment of the initial conditions [19].

### 1.3. Charmonium

By the time the CERN experiment NA38 was taking data on charmonium production in nuclear collisions, the possibility that formation of QGP will influence the final state yield of charmonium had been raised [20]. This important topic has undergone a significant evolution over the past 15 years. In fact the originally predicted charmonium suppression at SPS energy can turn to a charmonium enhancement at RHIC energies. By virtue of detailed balance, both dissociation and QGP based charmonium production channels must be considered. A requirement for dominating enhancement effect is a sufficient number of available open charm quark pairs in the QGP [21].

### 1.4. New state of matter

Based on these diverse experimental signatures, it is believed that a new form of matter, presumably quark matter, has been formed in relativistic nuclear collision experiments carried out at CERN-SPS [22]. Detailed analysis of strangeness production results in addition implies that a dense fireball of matter formed in these reactions expands explosively, supercools, and in the end encounters a mechanical instability which facilitates sudden break up into hadrons [23].

### 1.5. Strange hadron spectra and freeze-out

For the study presented in this paper the key point is that when sudden QGP breakup occurs, the spectra of hadrons are not formed at a range of stages in fireball evolution, but arise rather suddenly. Most importantly, particles of very different properties are produced by the same mechanism and thus are expected to have similar  $m_{\perp}$ -spectra, as is indeed observed [24]. The reported symmetry of the strange baryon and antibaryon spectra strongly suggests that the same reaction mechanism produces  $\Lambda$  and  $\bar{\Lambda}$  and  $\Xi$  and  $\bar{\Xi}$ . This is a surprising, but rather clear experimental fact, which we will interpret quantitatively in this paper.

When the momentum distributions of final state particles stop evolving during the fireball evolution, we speak of thermal freeze-out. Because a spectrum of strange hadrons includes directly produced and heavy resonance decay products, one can determine the freeze-out temperature and dynamical velocities of fireball evolution solely from the study of the precisely known shape of the particle spectra. We demonstrate this in some detail in section 4. The physical mechanism is that the freeze-out temperature determines the relative contribution of each decaying resonance while the shape of each decay contribution differs from the thermal shape, see section 2.

We note that we make in our analysis the tacit assumption that practically all decay products of resonances are thermally not re-equilibrated, which is equivalent to the assumption of sudden freeze-out. This is consistent with our finding that the  $m_{\perp}$  strange baryon and antibaryon distributions of  $\Lambda$ ,  $\bar{\Lambda}$ ,  $\Xi$ ,  $\bar{\Xi}$  froze out near to the condition at which the chemical particle yields were established.

One of the key objectives of this work is to present a comparison between thermal and chemical freeze-out analysis results for temperature, (explosion) collective velocity and other chemical and dynamical parameters. It is important to realize that particle spectra and yields are sensitive to the magnitude of collective matter flow, in which the produced particles are born, for somewhat different reasons:

- (i) in thermal analysis the collective flow combines with thermal freeze-out temperature to fix the shape of each particle spectrum, and temperature is also controlling the relative yield of contributing resonances—see previous paragraph for a tacit assumption that is relevant here—thus both  $T$  and  $v$  are fixed by the shape of  $m_{\perp}$  data;
- (ii) in chemical analysis the particle yields required are obtained by integrating spectral yields, with experimental acceptance in  $p_{\perp}, y$  implemented [18]. Since many particles have too small a particle momentum to be usually observed, the acceptance-cut yields used in chemical analysis depend quite sensitively on parameters which deform the soft part of the spectra without changing the number of produced particles, such as the flow velocity.

For these two reasons precise particle spectra and yields allow conclusions to be drawn about the proximity of thermal and chemical freeze-out conditions.

## 2. Thermal freeze-out analysis

In recent months experiment WA97 determined the absolute normalization of the published  $m_{\perp}$  distribution [24], and we took the opportunity to perform the spectral shape analysis and will compare our results with those obtained in chemical yield analysis [18] in order to check if the thermal and chemical freeze-out conditions are the same. Our analysis continues and this report gives its current status.

We report here a simultaneous analysis of absolute yield and shape of WA97 results of six  $m_{\perp}$ -spectra of  $\Lambda, \bar{\Lambda}, \Xi, \bar{\Xi}, \Omega + \bar{\Omega}, K_s^0 = (K^0 + \bar{K}^0)/2$  in four centrality bins, looking at all particles bin by bin. If thermal and chemical freeze-outs are identical, our present results must be consistent with earlier chemical analysis of hadron yields. Since the experimental data we study here are dominated by the shape of  $m_{\perp}$ -spectra and not by relative particle yields, our analysis is *de facto* comparing thermal and chemical freeze-outs.

We have found, as is generally believed and expected, that all hadron  $m_{\perp}$ -spectra are strongly influenced by resonance decays. Thus we apply standard procedure to allow for this effect [25, 26]. The final particle distribution is composed of directly produced particles and decay products:

$$\frac{dN_X}{dm_{\perp}} = \frac{dN_X}{dm_{\perp}}|_{\text{direct}} + \sum_{\forall R \rightarrow X+2+\dots} \frac{dN_X}{dm_{\perp}}|_{R \rightarrow X+2+\dots} \quad (1)$$

Here  $R(M, M_T, Y) \rightarrow X(m, m_T, y) + 2(m_2) + \dots$ , where we indicate by the arguments that only for the decay particle  $X$  do we keep the information about the shape of the momentum spectrum. We consider here only the two-body decay as no other contributing decays are known for hyperons and hard kaons. In detail, the decay contribution to the yield of  $X$  is:

$$\frac{dN_X}{dm_{\perp}^2 dy} = \frac{g_r b}{4\pi p^*} \int_{Y_-}^{Y_+} dY \int_{M_{T-}}^{M_{T+}} dM_T^2 J \frac{d^2 N_R}{dM_T^2 dY} \quad (2)$$

$$J = \frac{M}{\sqrt{P_T^2 p_T^2 - (ME^* - M_T m_T \cosh \Delta Y)^2}}.$$

We have used  $\Delta Y = Y - y$ , and  $\sqrt{s}$  is the combined invariant mass of the decay products other than particle  $X$  and  $E^* = (M^2 - m^2 - m_2^2)/2M$ ,  $p^* = \sqrt{E^{*2} - m^2}$  are the energy and momentum of the decay particle  $X$  in the rest frame of its parent. The limits on the integration are the maximum values accessible to the decay product  $X$ :

$$Y_{\pm} = y \pm \sinh^{-1} \left( \frac{p^*}{m_T} \right)$$

$$M_{T\pm} = M \frac{E^* m_T \cosh \Delta Y \pm p_T \sqrt{p^{*2} - m_T^2} \sinh^2 \Delta Y}{m_T^2 \sinh^2 \Delta Y + m^2}.$$

The theoretical primary particle spectra (both those directly produced and parents of decay products) are derived from the Boltzmann distribution by Lorenz-transforming from a flowing intrinsic fluid element to the CM frame, and integrating over allowed angles between particle direction and local flow.

We introduce two velocities: a local flow velocity  $v$  of fireball matter from where particles emerge, and hadronization surface (breakup) velocity which we refer to as  $v_f^{-1} \equiv dt_f/dx_f$ . Particle production is controlled by the effective volume element, which comprises

$$dS_{\mu} p^{\mu} = d\omega \left( 1 - \frac{\vec{v}_f^{-1} \cdot \vec{p}}{E} \right) \quad d\omega \equiv \frac{d^3 x d^3 p}{(2\pi)^3}. \quad (3)$$

The Boltzmann distribution we adopt thus has the form

$$\frac{d^2 N}{dm_T dy} \propto \left( 1 - \frac{\vec{v}_f^{-1} \cdot \vec{p}}{E} \right) \gamma m_T \cosh y e^{-\gamma \frac{E}{T} \left( 1 - \frac{\vec{v} \cdot \vec{p}}{E} \right)} \quad (4)$$

where  $\gamma = 1/\sqrt{1 - v^2}$ .

The normalization for each hadron type  $h = X, R$  is

$$N^h = V_{\text{QGP}} \prod_{i \in h}^n \lambda_i \gamma_i.$$

Here we use the chemical parameters  $\lambda_i, \gamma_i$   $i = q, s$  which are as defined in [18], and commonly used to characterize relative and absolute abundances of light and strange quarks.

Since the particle spectra we consider have a good relative normalization, only one parameter is required for each centrality in order to describe the absolute normalization of all six hadron spectra. This is important for two reasons:

- (a) we can check if the volume from which strange hadrons are emitted grows with centrality of the collision as we expect;
- (b) we can determine which region in  $m_{\perp}$  produces the excess of  $\Omega$  noted in the chemical fit [18] is coming from.

However, since the normalization  $V_{\text{QGP}}$  common for all particles at given centrality comprises additional experimental acceptance normalization, we have not determined the value of the fireball emission volume at each centrality. Hence we will be presenting the volume parameter as function of centrality in arbitrary units.

The best thermal and chemical parameters which minimize the total relative error  $\chi_T^2$  at a given centrality:

$$\chi_T^2 = \sum_i \left( \frac{F_i^{\text{theory}} - F_i}{\Delta F_i} \right)^2$$

for all experimental measurement points  $F_i$  having measurement error  $\Delta F_i$  are determined by considering simultaneously for the results of experiment WA97 [24] i.e.  $K_s^0$ ,  $\Lambda$ ,  $\bar{\Lambda}$ ,  $\Xi$ ,  $\bar{\Xi}$ ,  $\Omega$  +  $\bar{\Omega}$ . We have checked the validity of the statistical analysis by the usual method, i.e. omission of some data in the fit.

Only in the case of kaons do we find any impact of such a procedure. Noting that the statistical error of kaon spectra is the smallest, we have established how a systematic error, which could be for kaons greater than the statistical error, would influence our result. For this purpose we assign to  $K^0$  experimental results in most of our analysis an ‘error’ which we arbitrarily have chosen to be five times greater than the statistical error. In this way the weight of the kaon spectra in the analysis is greatly reduced. In the first result (see figure 1 below) we present both results: the standard  $K^0$  error and the enlarged error. We see that while in individual results some change can occur, overall the physical results of both analyses are consistent. Thus we can trust in the combined study of hyperon and kaon data. This conclusion is reaffirmed in section 4, where we will see that the minimization of  $\chi_T^2$  involves more or less pronounced minima, depending on the error size of the kaon spectra, see figure 11. In most calculations we present in this paper we will be using, unless otherwise stated, hyperon results combined with the kaon data with five times enlarged statistical error. We believe that in this way we will err on the conservative side in our physical conclusions.

### 3. Overview of the results

We show here a slate of results obtained within the approach outlined above. First we address the parameters determining the shape of the  $m_\perp$  distributions, that is  $T$ ,  $v$ ,  $v_f$ .

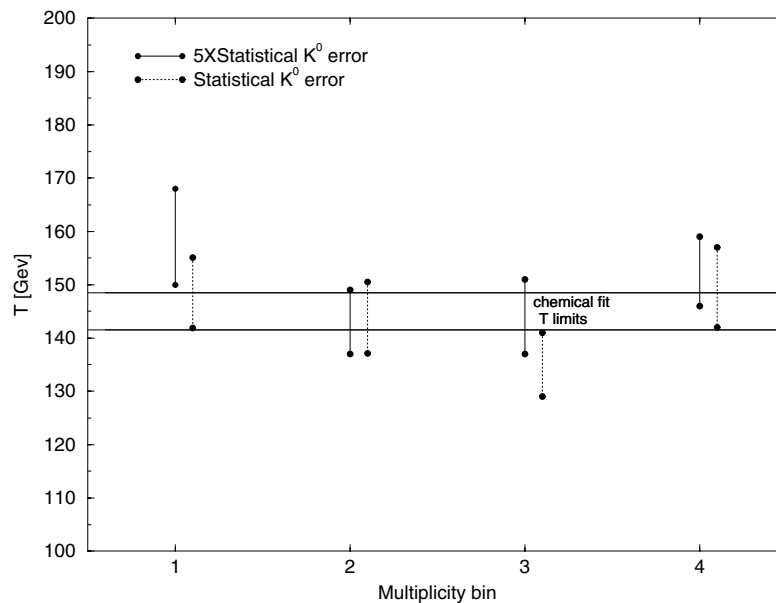


**Figure 1.** Thermal freeze-out temperature  $T$  for different centrality bins compared to chemical freeze-out analysis shown by horizontal solid lines. Original statistical error is used in the dotted results, five times statistical error for kaon data is used in solid vertical lines, see text.



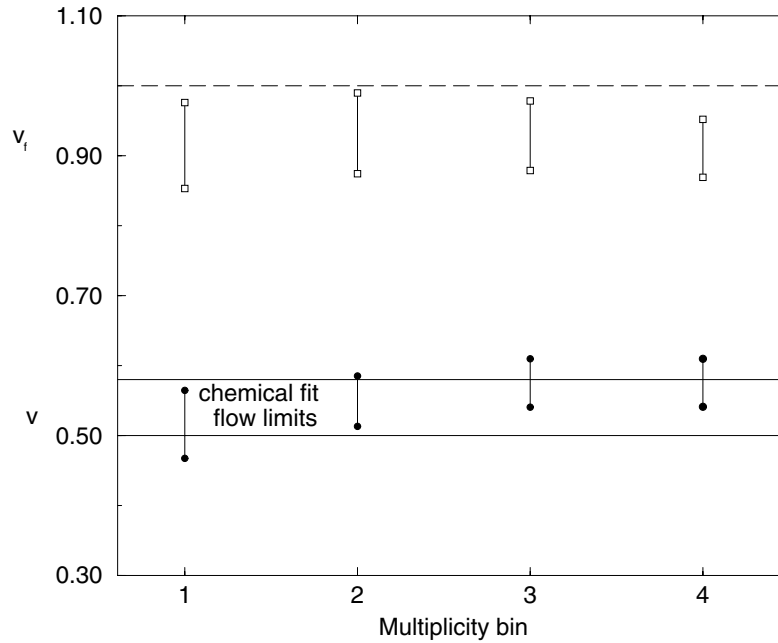


**Figure 2.** Thermal freeze-out flow velocity  $v$  (top) and break up (hadronization) velocity  $v_f$  for different centrality bins. Upper limit  $v_f = 1$  (dashed line) and chemical freeze-out analysis limits for  $v$  (solid lines) are also shown.

We show in figure 1 the freeze-out temperature  $T$  of the  $m_\perp$  spectra as a function of the centrality bin. The horizontal lines delineate the range of the results of the most recent chemical freeze-out analysis, see [18].

It is reassuring that we find a result consistent with the purely chemical analysis of data that included non-strange hadrons [18]. There is no indication of a significant or systematic change of  $T$  with centrality. This is consistent with the belief that the formation of the new state of matter at CERN is occurring in all centrality bins explored by the experiment WA97. Only most peripheral interactions produce a change in the pattern of strange hadron production [27]. The (unweighted) average of all results shown in figure 1 produces a freeze-out temperature at the upper boundary of the pure chemical freeze-out analysis result,  $T \simeq 145$  MeV. It should be noted that in chemical analysis  $v_f = v$  [18], which may be the cause of this slight difference between current analysis average and the earlier purely chemical analysis result.

The magnitudes of the collective expansion velocity  $v$  and the break-up (hadronization) speed parameter  $v_f$  are presented in figure 2. For  $v$  (lower part of the figure) we again see consistency with earlier chemical freeze-out analysis results, and there is no confirmed systematic trend in the behaviour of this parameter as function of centrality.

Though within the experimental error, one could argue on inspecting figure 2 that there is a systematic increase in transverse flow velocity  $v$  with centrality and thus size of the system. This is expected, since the more central events comprise greater volume of matter, which allows more time for development of the flow. Interestingly, it is in  $v$  and not  $T$  that we find the slight change of spectral slopes noted in the presentation of the experimental data [24].

The value of the break-up (hadronization) speed parameter  $v_f = 1/(\partial t_f/\partial r_f)$  shown in the top portion of figure 2 is close to the velocity of light which is highly consistent with the picture



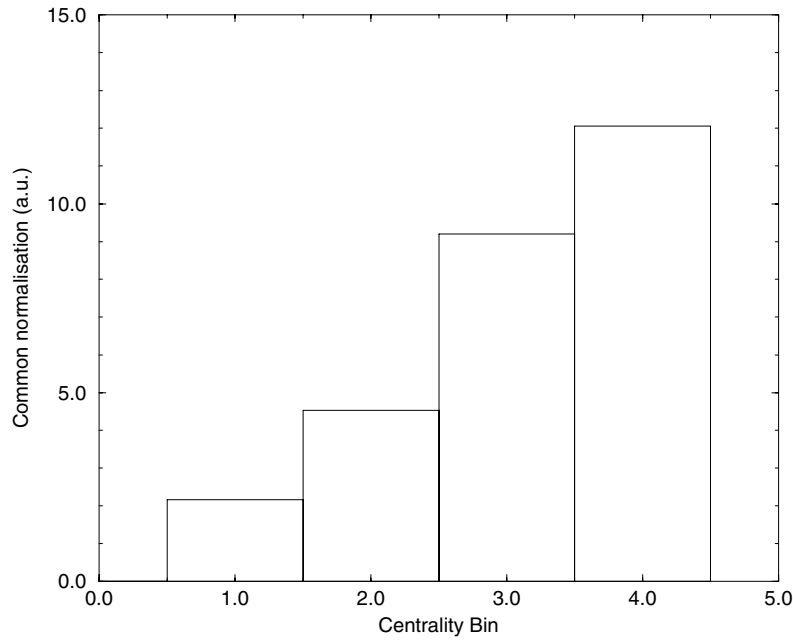


**Figure 3.** Hadronization volume (arbitrary units) for different centrality bins.

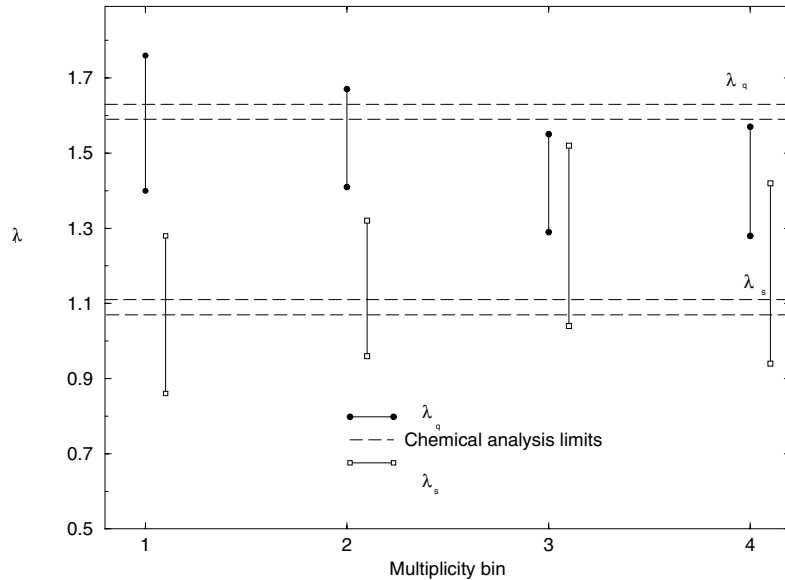


**Figure 4.** Thermal analysis chemical quark fugacity  $\lambda_q$  (top) and strange quark fugacity  $\lambda_s$  (bottom) for different centrality bins compared to the chemical freeze-out analysis results.

of a sudden breakup of the fireball. This hadronization surface velocity  $v_f$  was in the earlier chemical fit set to be equal to  $v$ , as there was not enough sensitivity in purely chemical fit to determine the value of  $v_f$ .

Unlike the temperature and two velocities, the overall normalization of hadron yields,  $V^h$ , must be, and is, strongly centrality dependent as is seen in figure 3. This confirms in

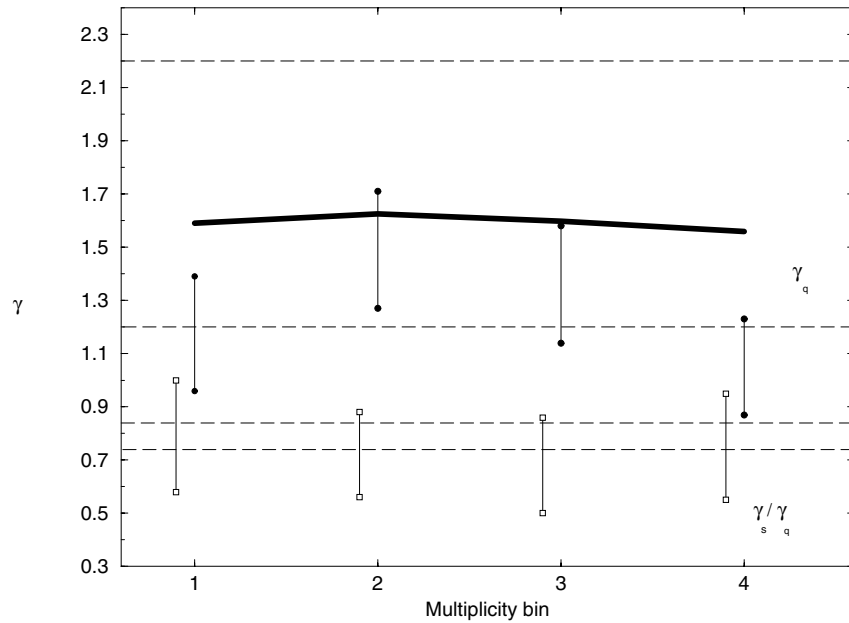


**Figure 5.** Thermal analysis chemical quark abundance parameter  $\gamma_q$  (top) and  $\gamma_s/\gamma_q$  (bottom) for different centrality bins compared with the chemical freeze-out analysis. Thick line: upper limit due to pion condensation.

a quantitative way the belief that the entire available fireball volume is available for hadron production. The strong increase in the volume by a factor of six is qualitatively consistent with a geometric interpretation of the collision centrality effect. Not shown is the error propagating from the experimental data which is strongly correlated to the chemical parameters discussed next. This systematic uncertainty is another reason we do not attempt an absolute unit volume normalization.

The four chemical parameters  $\lambda_q$ ,  $\lambda_s$ ,  $\gamma_q$ ,  $\gamma_s/\gamma_q$  are shown in figures 4 and 5. These parameters determine along with  $V^h$  the final particle yield. Since we have five parameters determining the normalization of six strange hadron spectra, and as discussed we reduce the statistical weight of kaons, there is obviously a lot of correlation between these four quantities, and thus the error bar which reflects this correlation is significant.

The chemical fugacities  $\lambda_q$  and  $\lambda_s$  shown in figure 4 do not exhibit a systematic centrality dependence. This is consistent with the result we found for  $T$  in that the freeze-out properties of the fireball are seen to be for temperature and chemical potential values independent of the size of the fireball. Comparing to the earlier chemical freeze-out result in figure 4 one may argue that there is a systematic downward deviation in  $\lambda_q$ . However, this could be caused by the fact that the chemical freeze-out analysis allowed for isospin-asymmetric  $\Xi^-(dss)$  yield [18], while our present analysis is not yet distinguishing light quarks.

The ratio  $\gamma_s/\gamma_q$  shown in the bottom portion of figure 5 is systematically smaller than unity, consistent with many years of prior analysis: when  $\gamma_q = 1$  is tacitly chosen, this ratio is the value of  $\gamma_s$  in analysis of strange baryons. We have not imposed a constraint on the range of  $\gamma_q$  (top of figure 5) and thus values greater than the pion condensation point  $\gamma_q^* = e^{m_\pi/2T} \simeq 1.65$  (thick line) can be expected, but in fact do not arise.

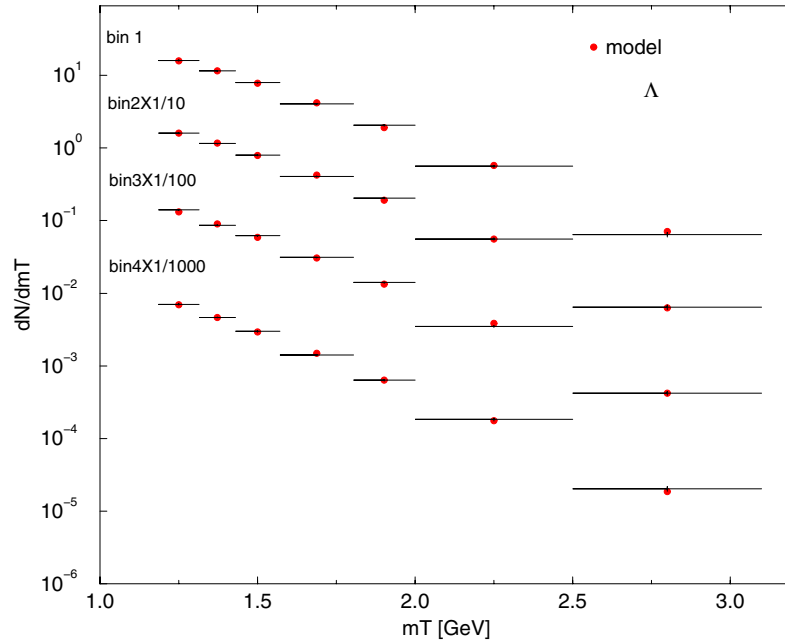


**Figure 6.** Thermal analysis  $m_T$  spectra:  $\Lambda$ .

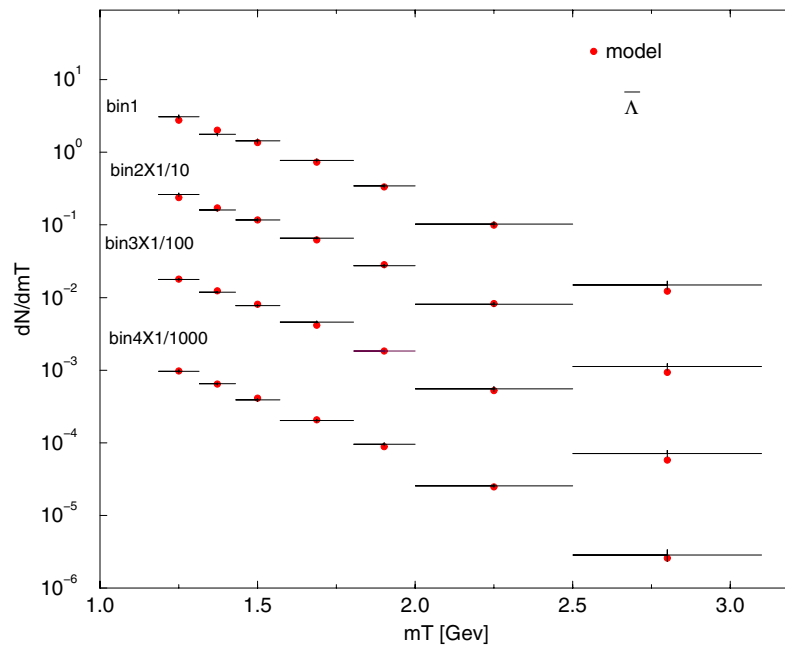


**Figure 7.** Thermal analysis  $m_T$  spectra:  $\bar{\Lambda}$ .

It is important to explicitly check how well the particle  $m_\perp$  spectra are reproduced. We group all bins in one figure and show in figures 6, 7, 8 and 9 in sequence  $\Lambda$ ,  $\bar{\Lambda}$ ,  $\Xi$  and  $\bar{\Xi}$ . It is important to note that there are no significant or systematic deviations comparing the model to the data. Overall, the description of the shape of the spectra is very satisfactory.

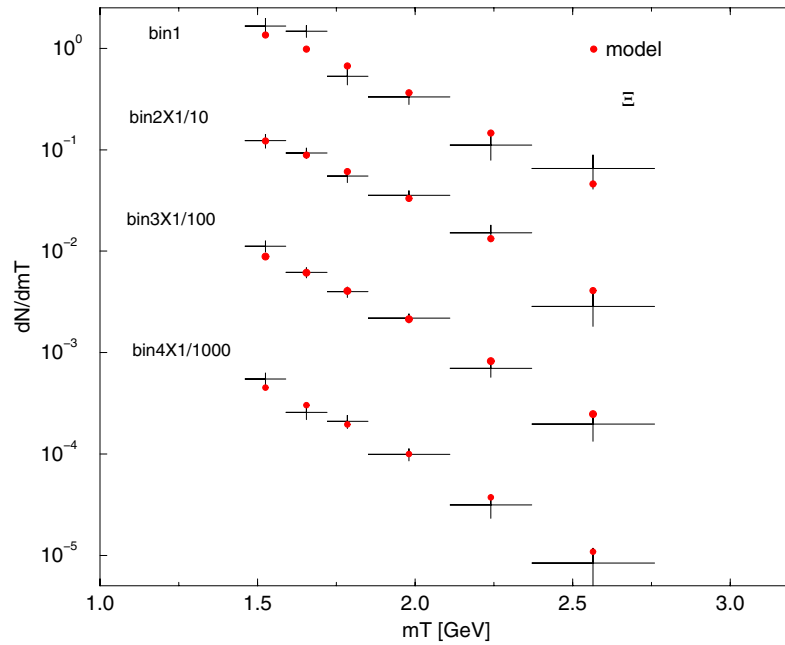


**Figure 8.** Thermal analysis  $m_T$  spectra:  $\Xi$ .

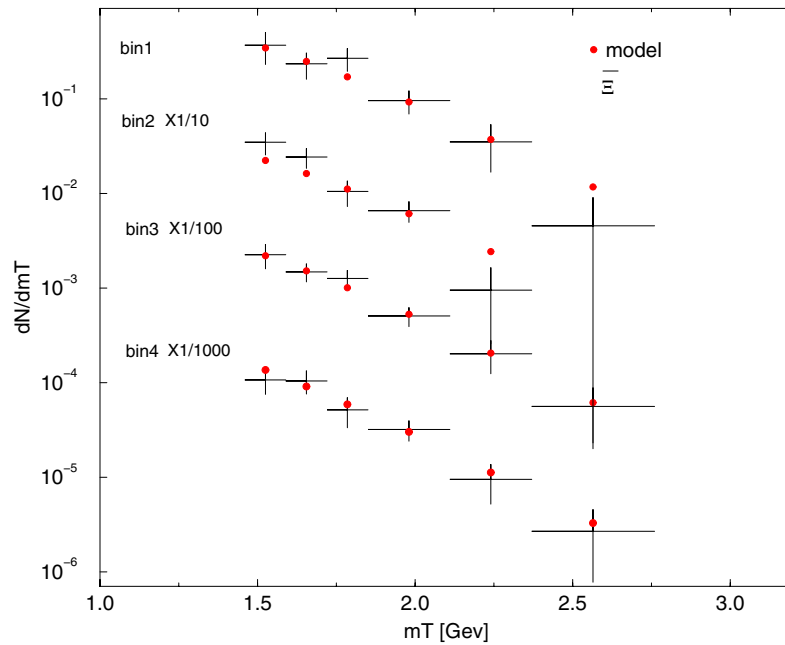


**Figure 9.** Thermal analysis  $m_T$  spectra:  $\Xi$ .

We also describe the  $K^0$  data extremely well, especially in the  $m_\perp$  range which is the same as that for hyperons considered earlier, as is seen in figure 10. We recall that these results were obtained reducing the statistical significance of kaon data, and thus the conclusion is that hyperons predict both the abundance and shape of kaon spectra. Moreover, all the strange hadron spectra can be well described within the model we have adopted.

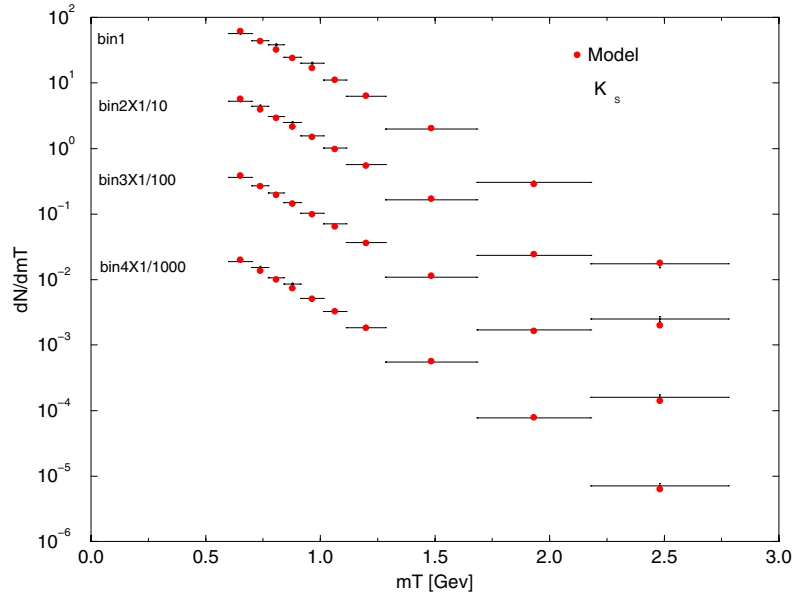


**Figure 10.** Thermal analysis  $m_T$  spectra:  $K_s^0$ .

#### 4. Statistical significance of the results presented

We have analysed the validity and consistency of our data analysis by exploring  $\chi^2/DoF$  profiles. These are obtained by fixing the value of one of the parameters (we consider  $T_f$ ,  $v$ ,  $\partial t_f/\partial r_f = 1/v_f$ ) and computing the related  $\chi_T^2/DoF$ , the total error divided by the degrees of freedom. These are the number of measurements minus the number of parameters,  $DoF$  is typically 33 in this data analysis. All curves must have the same  $\chi_T^2/DoF$  at the minimum and this minimum must point to the value of parameters we report. For the temperature  $T$  we produced two results shown in figure 11, in the bottom section for experimental (statistical)  $K^0$  measurement error, and in the top part for the five times enlarged error. We recall that both results are presented in figure 1. We note that there is a pronounced  $\chi_T^2/DoF$  minimum shown (on logarithmic scale) for all eight results of which the average value is at  $T = 145$  MeV.

We show in figure 12 the profile of  $\chi_T^2/DoF$  for the collective flow velocity  $v$  (top) and the freeze-out surface  $\partial t_f/\partial r_f = 1/v_f$  motion (bottom) being fixed. These minima can be shown on a linear scale. We note a mild secondary minimum in the region  $v \simeq 0.25$ – $0.35$ . However, the minima we find at  $v = 0.5$ – $0.58$  are by far more significant.  $\partial t_f/\partial r_f = 1/v_f$  is converging to a sharp minimum seen in bottom portion of figure 12 at a value consistent with the sudden breakup scenario. It is necessary to include  $\partial t_f/\partial r_f = 1/v_f$  along with  $v$  in the analysis to find this result, which was not always done in other studies of particle spectra.

#### 5. Omega spectra

In figure 13 all four centrality bins for the sum  $\Omega + \bar{\Omega}$  are shown. We see that we systematically under-predict the two lowest  $m_\perp$  data points. Some deviation at high  $m_\perp$  may be attributable to acceptance uncertainties, also seen in the the  $\Xi$  result presented earlier in figure 9. We recall

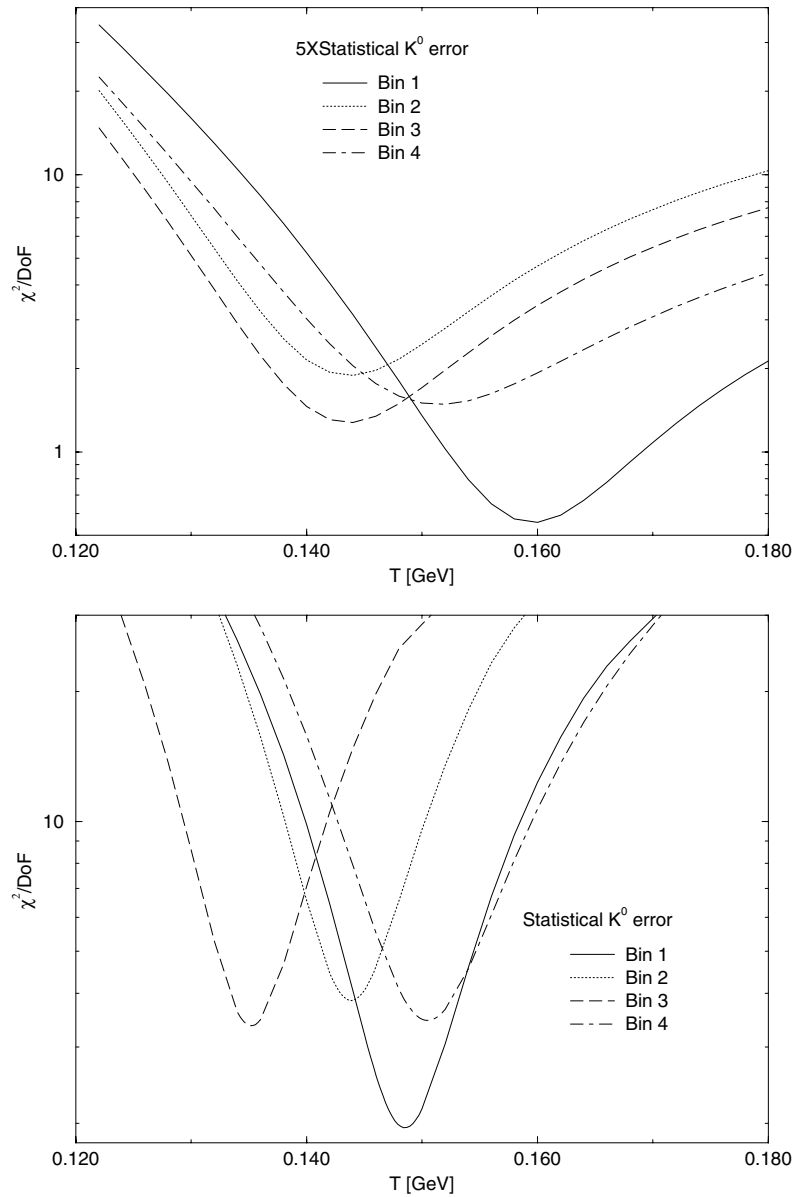


**Figure 11.** The total error divided by degrees of freedom for different centrality bins, shown as function of (fixed) freeze-out temperature  $T$ . Bottom: for the experimental value of the (statistical)  $K^0$  error; top: for the five times enlarged kaon data statistical errors.

that there is a disagreement with the omega yields in the chemical analysis, which thus does not include in the analysis the production of  $\Omega$ . In the analysis presented here we see that this disagreement is arising at low momentum.

The low- $m_\perp$  anomaly also explains why the inverse  $m_\perp$  slopes for  $\Omega, \bar{\Omega}$  are smaller than the values seen in all other strange (anti)hyperons. One can presently only speculate about the processes which contribute to this anomaly. We note that the 1–2s.d. deviations in the low- $m_\perp$ -bins of the  $\Omega + \bar{\Omega}$  spectrum translate into 3s.d. deviations from the prediction of the chemical analysis. This is mainly a consequence of the fact that after summing over centrality and  $m_\perp$ ,

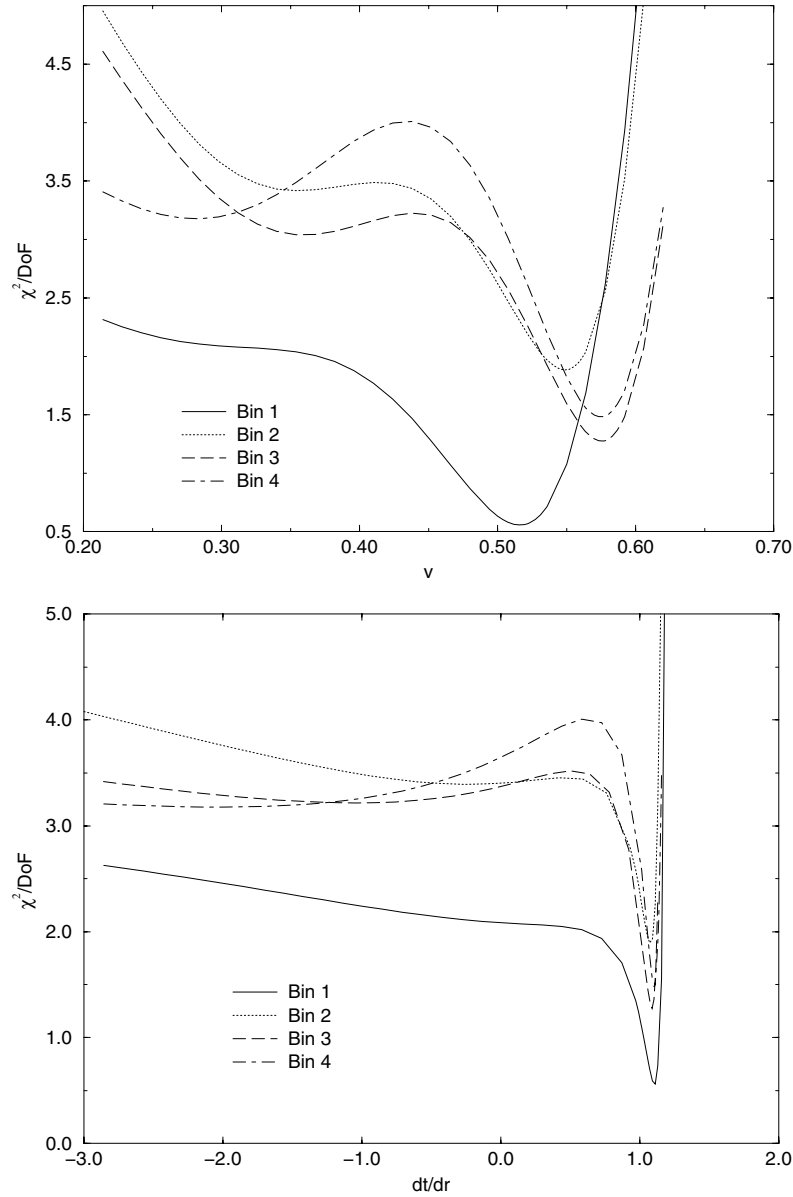


**Figure 12.** The total error divided by degrees of freedom for different centrality bins, shown as a function of (fixed) flow velocity  $v$  (top) and for (fixed) freeze-out surface  $\partial t_f/\partial r_f = 1/v_f$  dynamics (bottom).

the statistical error which dominates the  $\Omega + \bar{\Omega}$  spectra becomes relatively small, and as can be seen the low- $m_\perp$  excess practically doubles the  $\Omega$  yield.

## 6. Final remarks

Our thermal freeze-out analysis confirms that CERN-SPS results decisively show interesting and new physics, and confirms the reaction picture of a suddenly hadronizing QGP-fireball with both chemical and thermal freeze-out being the same. In our view driven by internal pressure, a quark



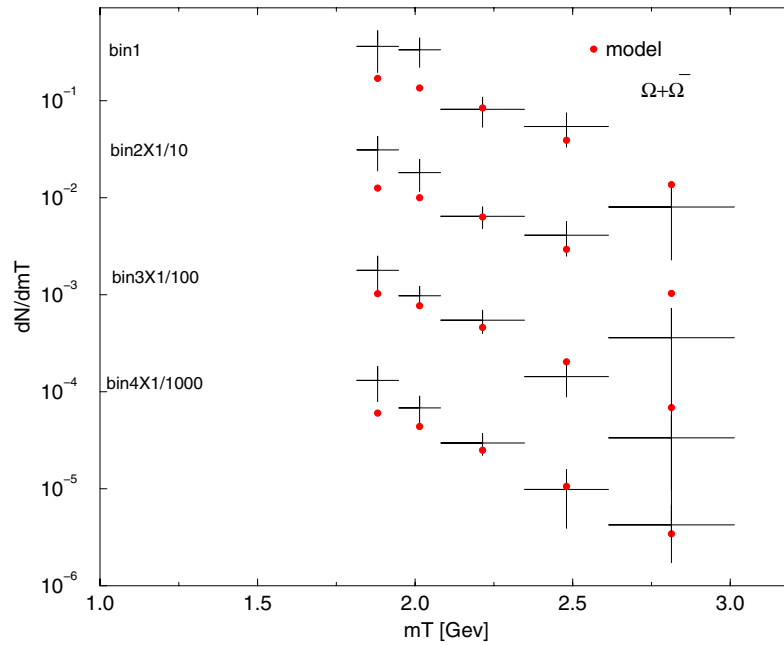


**Figure 13.** Thermal analysis  $m_T$  spectra:  $\Omega + \bar{\Omega}$ .

gluon fireball expands and ultimately a sudden breakup (hadronization) into final state particles occurs which reaches detectors without much, if any, further rescattering. The required sudden fireball breakup arises as the fireball supercools, and in this state encounters a strong mechanical instability [23]. Note that deep supercooling requires a first-order phase transition.

The remarkable similarity of  $m_{\perp}$  spectra reported by the WA97 experiment is interpreted by a set of freeze out parameters, and we see that production mechanism of  $\Lambda$ ,  $\bar{\Lambda}$ , and  $\Xi$ ,  $\bar{\Xi}$  is the same. This symmetry, including matter–antimatter production, is an important cornerstone of the claim that the strange antibaryon data can only be interpreted in terms of direct particle emission from a deconfined phase.

The reader must remember that in the presence of conventional hadron collision based physics, the production mechanism of antibaryons is quite different from that of baryons and a similarity of the  $m_{\perp}$  spectra is not expected. Moreover, even if QGP is formed, but a equal phase of confined particles is present, the annihilation of antibaryons in the baryon-rich medium created at CERN-SPS energy would deplete more strongly antibaryon yields, in particular so at small particle momentum, with the more abundant baryons remaining less influenced. This effect is not observed [24].

Similarity of  $m_{\perp}$ -spectra does not at all imply in our argument a similarity of particle rapidity spectra. As hyperons are formed at the fireball breakup, any remaining longitudinal flow present among fireball constituents will be imposed on the product particle, thus  $\Lambda$  spectra containing potentially two original valence quarks are stretched in  $y$ , which  $\bar{\Lambda}$ - $y$  spectra are not, as they are made from newly formed particles. All told, one would expect that anti-hyperons can appear with a thermal rapidity distribution, but hyperons will not. But both have the same thermal-explosive collective flow controlled shape of  $m_{\perp}$  spectra.

We have shown that the thermal freeze-out condition for strange hadrons ( $K_s^0$ ,  $\Lambda$ ,  $\bar{\Lambda}$ ,  $\Xi$ ,  $\bar{\Xi}$ ) agrees within error with chemical freeze-out and we have confirmed the freeze-out temperature

$T \simeq 145$  MeV. These findings about the similarity of thermal and chemical freeze-out were controversial when the experimental single particle spectra were lacking precision, since pion spectra and two particle correlation analysis did not yield this result. However, this paper studies the precise hyperon and kaon  $m_{\perp}$  spectra which reach to relatively low  $p_{\perp}$  and compares with definitive chemical analysis of SPS data. The two-particle correlation analysis involves pions, which, unlike the strange hadrons here considered, are potentially witnesses to other physics than the properties of dense and hot quark gluon phase.

We were able to determine the freeze-out surface  $1/v_f = \partial t_f / \partial r_f$  dynamics and have shown that the break-up velocity  $v_f$  is nearly the velocity of light, as would be expected in a sudden breakup of a QGP fireball. A study with  $\partial t_f / \partial r_f$  has not been previously considered, and only collective flow is included in the description of the particle source. In our analysis we find a slight increase of the transverse expansion velocity with the size of the fireball volume, but consistently  $v \leq 1/\sqrt{3}$ .

We have reproduced the strange particle spectra in all centrality bins. Our findings rely strongly on results obtained by WA97 at smallest accessible particle momentum, and this stresses the need to reach to the smallest possible  $p_{\perp}$  in order to be able to explore the physics of particle freeze-out from the deconfined region. Moreover, we demonstrated that the experimental production data of  $\Omega + \bar{\Omega}$  has a noticeable systematic low  $p_{\perp}$  enhancement anomaly present in all centrality bins. This result shows that it is not a different temperature of freeze-out of  $\Omega + \bar{\Omega}$  that leads to more enhanced yield, but a soft momentum secondary source which contributes almost equal number of soft  $\Omega + \bar{\Omega}$  compared to the systematic yield predicted by the other strange hadrons.

## Acknowledgments

Supported by a grant from the US Department of Energy, DE-FG03-95ER40937.

*Note added.* We have been made aware by the referee that an analysis of the  $m_{\perp}$  spectra for high-energy collisions has been carried out recently [28]. This work reaches, for elementary high-energy processes, similar conclusions to those we have presented regarding the identity of chemical and thermal freeze-out. The higher freeze-out temperature found is also consistent with our results, considering that in nuclear collisions significant supercooling occurs [23].

## References

- [1] Itoh N 1970 *Prog. Theor. Phys.* **44** 291
- [2] Carruthers P 1973 *Collective Phenomena* **1** 147
- [3] Iachello F, Langer W D and Lande W D 1974 *Nucl. Phys. A* **219** 612
- [4] Collins J C and Perry M J 1975 *Phys. Rev. Lett.* **34** 1353
- [5] Hagedorn R 1985 How we got to QCD matter from the hadron side by trial and error *Quark Matter'84* (*Springer Lecture Notes in Physics*, vol 221) ed K Kajantie (Berlin: Springer) p 53
- [6] Chin S A 1978 *Phys. Lett. B* **78** 552
- [7] Feinberg E L 1976 *Nuovo Cimento A* **34** 391
- [8] Shuryak E V 1978 *Phys. Lett. B* **78** 150
- [9] Domokos G and Goldman J I 1981 *Phys. Rev. D* **23** 203
- [10] Rafelski J 1981 Extreme states of nuclear matter *Future Relativistic Heavy Ion Experiments* ed R Bock and R Stock, GSI Report 1981-6, pp 282–324

- Rafelski J and Hagedorn R 1981 From hadron gas to quark matter II *Statistical Mechanics of Quarks and Hadrons* ed H Satz (Amsterdam: North-Holland) pp 253–72
- Rafelski J 1981 Hot hadronic matter *New Flavor and Hadron Spectroscopy* ed J Tran Thanh Van (Paris: Editions Frontières) pp 619–32
- Rafelski J 1982 *Nucl. Phys. A* **374** 489c
- [11] Rafelski J and Müller B 1982 *Phys. Rev. Lett.* **48** 1066
- Rafelski J and Müller B 1986 *Phys. Rev. Lett.* **56** 2334E
- Koch P, Müller B and Rafelski J 1986 *Z. Phys. A* **324** 453
- [12] Rafelski J 1982 *Phys. Rep.* **88** 331
- [13] Rafelski J and Danos M 1983 *Perspectives in High Energy Nuclear Collisions*, NBS-IR 83-2725 Monograph, US Department of Commerce, National Bureau of Standards
- Updated version appeared in Heiss D (ed) 1985 *Nuclear Matter under Extreme Conditions (Springer Lecture Notes in Physics, vol 231)* (Berlin: Springer) pp 362–455
- [14] Koch P and Rafelski J 1985 *Nucl. Phys. A* **444** 678
- [15] Koch P, Müller B and Rafelski J 1986 *Phys. Rep.* **142** 167
- [16] Antinori F *et al* WA97 Collaboration 2000 *Nucl. Phys. A* **663** 717
- Andersen E *et al* WA97 Collaboration 1998 *Phys. Lett. B* **433** 209
- Andersen E *et al* WA97 Collaboration 1999 *Phys. Lett. B* **449** 401
- [17] Antinori F *et al* WA97 Collaboration 1999 *Eur. Phys. J. C* **11** 79
- [18] Letessier J and Rafelski J 2000 *Int. J. Mod. Phys. E* **9** 107 and references therein
- For data and analysis update, see Rafelski J, Letessier J and Torrieri G 2001 *Preprint* nucl-th/0104042
- [19] Hamieh S, Letessier J and Rafelski J 2000 *Phys. Rev. C* **62** 064901
- [20] Matsui T and Satz H 1986 *Phys. Lett. B* **178** 416
- [21] Thews R L, Schroedter M and Rafelski J 2001 *Phys. Rev. C* **63** 054905
- Thews R L, Schroedter M and Rafelski J 2001 *J. Phys. G: Nucl. Part. Phys.* **27** 715
- [22] See the web page: <http://www.cern.ch/CERN/Announcements/2000/NewStateMatter/>
- Text of the scientific consensus view of the spokesmen of CERN experiments is also available as: Heinz U and Jacob M (compilers) 2000 Evidence for a new state of matter: an assessment of the results from the CERN Lead Beam Programme *Preprint* nucl-th/0002042
- [23] Rafelski J and Letessier J 2000 *Phys. Rev. Lett.* **85** 4695
- [24] Antinori F *et al* WA97 Collaboration 2000 *Eur. Phys. J. C* **14** 633 and private communication.
- [25] Schnedermann E, Sollfrank J and Heinz U 1995 *NATO ASI series B, Physics* **303** 175
- [26] Anisovich V V, Kobrinsky M N, Nyiri J and Shabelski Y 1985 *Quark Model and High Energy Collisions* (Singapore: World Scientific)
- [27] Kabana S *et al* NA52 Collaboration 1999 *Nucl. Phys. A* **661** 370c
- Kabana S *et al* NA52 Collaboration 1999 *J. Phys. G: Nucl. Part. Phys.* **25** 217
- [28] Becattini F, Bellucci L and Passaleva G 2001 *Nucl. Phys. Proc. Suppl.* **92** 137–48